

## INFLUENCE OF CHEMICAL MODIFICATION OF THE SOLUBLE SODIUM SILICATE ON THE ZETA POTENTIAL OF THE COLLOIDAL PARTICLES IN A “SOLUBLE SODIUM SILICATE – ESTER HARDENER” GELLING SYSTEM

### WPŁYW MODYFIKACJI CHEMICZNEJ ROZPUSZCZALNEGO KRZEMIANU SODU NA POTENCJAŁ ZETA CZĄSTECZEK KOLOIDALNYCH W UKŁADZIE ŻELUJĄCYM „ROZPUSZCZALNY KRZEMIAN SODU – UTWARDZACZ ESTROWY”

Andrzej Baliński

Instytut Odlewnictwa, ul. Zakopiańska 73, 30-418 Kraków

#### **Abstract**

The article presents how to perform a chemical modification of the soluble sodium silicate with morphoactive, organic compounds. An attempt was made to determine the effect of chemical modifiers of the soluble sodium silicate on its physicochemical and structural properties. The kinetics of changes in the Zeta potential of a "chemically modified soluble sodium silicate – ester hardener" gelling system was described.

**Key words:** soluble sodium silicate, chemical modification, Zeta potential

#### **Streszczenie**

W artykule przedstawiono sposób modyfikacji chemicznej uwodnionego krzemianu sodu za pomocą morfoaktywnych związków organicznych. Podjęto próbę określenia wpływu modyfikatorów chemicznych uwodnionego krzemianu sodu na jego właściwości fizykochemiczne i strukturalne. Opisano kinetykę zmian wartości potencjału Zeta żelującego układu „modyfikowany chemicznie uwodniony krzemian sodu – utwardzacz estrowy”.

**Słowa kluczowe:** uwodniony krzemian sodu, modyfikacja chemiczna, potencjał Zeta

## **Introduction**

Soluble sodium silicate having the general formula  $x\text{Na}_2\text{O} \cdot y\text{SiO}_2$  is one of the most common inorganic binders. In the foundry industry, soluble sodium silicate is a binder used to make sand moulds and cores for castings from the ferrous and nonferrous metals. In the European countries, the share of castings made in these sands, hardened with liquid esters or carbon dioxide, is up to 30% of the total production. The advantage of moulding sands with the soluble sodium silicate is high heat resistance of moulds and cores, which is particularly important for medium and heavy castings, and also absence

of the emission of toxic gases during mould making and pouring. In addition to these environmental and technological advantages, there are also important economic considerations. Moulding sands with the soluble sodium silicate are much cheaper than their counterparts prepared with resin binders.

However, compared to theresin-bonded moulding sands, besides some obvious advantages, moulding sands with the soluble sodium silicate have also several disadvantages, to mention only the excessively high residual strength, and hence the inferior knocking out properties and difficult reclamation of the used sand, as well as the low initial strength (especially cohesive). Another disadvantage of this type of moulding sand is also the formation of sinters resulting from the tendency of  $\text{Na}_2\text{O} - \text{SiO}_2$  to react with quartz sand at elevated temperatures. The sintering process can be reduced by reducing the amount of binder in the moulding sand and by suitable modification of the *binder – sand grain* interface. Reducing the amount of silicate binder is possible only if its binding properties can be improved.

It is the fact well-known that the binding properties of organic binders are improved due to the presence of the functional groups like  $-\text{NH}_2$ ,  $-\text{COOH}$ ,  $-\text{CONH}_2$  and others [1–3]. It was recognized that the properties of the soluble sodium silicate can be improved by the introduction of modifiers containing these functional groups.

The used modifiers tend to form with the soluble sodium silicate an *IPN (Interpenetrating Polymer Networks)* type network, which is a mutually interpenetrating polymer network. The consequence is the reduced “final strength” of moulding sand produced with the modified solution of soluble silicate. Regardless of the influence of the *IPN* network, the strength properties of silica gel are also affected by the characteristics of its structure associated with the hardening kinetics, depending on the kinetics of changes in the Zeta potential of the particles in a “soluble sodium silicate – ester hardener” gelling system.

## **Methodology of measurements**

Chemical modification of soluble sodium silicate was performed with the organic morphoactive compounds C1, C3 and C6. The chemical modification consisted in introducing to an autoclave the sodium silicate glaze with the modulus  $M = 3.1$ , and demineralised water. The autoclaving process was carried out under constant conditions, i.e. at a temperature of 160°C to 180°C and a pressure from 0.6 MPa to 0.8 MPa. To obtain the required amount of the soluble sodium silicate, for the operation of concentration and to confirm the reproducibility of the results, several dissolution tests were performed on the sodium silicate glaze. The duration of the dissolution process was approximately 3 hours. The solution in the autoclave was decompressed, and then the autoclave was evacuated. The soluble sodium silicate after the autoclaving process and concentration was subjected to filtration.

The soluble sodium silicate had a density of 1.248 g/cm<sup>3</sup> and molar modulus of about 3.0. This solution was subjected to correction of the modulus  $M$  to about 2.0 and was concentrated to a density of about 1.5 g/cm<sup>3</sup>. Chemical modification was carried out before the concentration step, introducing to the soluble sodium silicate solution with a corrected modulus, the morphologically active agents C1, C3 and C6, added in an amount of 0.1%, 0.5% and 1.0%, calculated in relation to the total amount of oxides

present in the soluble sodium silicate ( $\text{Na}_2\text{O} + \text{SiO}_2$ ). The characteristics of the obtained types of the sodium silicate are shown in Table 1.

*Table 1. Characteristics of the basic physico-chemical properties of chemically modified types of the soluble sodium silicate and of a standard chemically non-modified soluble sodium silicate (S)*

*Tabela 1. Charakterystyka podstawowych właściwości fizykochemicznych modyfikowanych chemicznie rodzajów uwodnionego krzemianu sodu oraz wzorcowego, niemodyfikowanego chemicznie uwodnionego krzemianu sodu (S)*

Type of soluble sodium silicate	Type of modifier	Modifier content, wt. %	Oxides content, wt. %		Modulus, M	Density, g/cm <sup>3</sup>
			$\text{Na}_2\text{O}$	$\text{SiO}_2$		
C1-0.1	C1	0.1	13.89	29.35	2.18	1.501
C1-0.5	C1	0.5	13.68	29.62	2.24	1.501
C1-1.0	C1	1.0	13.79	29.47	2.20	1.501
C3-0.1	C3	0.1	14.56	28.32	2.00	1.500
C3-0.5	C3	0.5	14.37	28.59	2.05	1.501
C3-1.0	C3	1.0	14.41	28.84	2.06	1.500
C6-0.1	C6	0.1	14.05	28.91	2.12	1.501
C6-0.5	C6	0.5	14.02	29.06	2.13	1.500
C6-1.0	C6	1.0	13.92	28.58	2.11	1.501
S	—	—	14.53	28.89	2.05	1.501

Under the effect of water, the surface of silicon dioxide and of other insoluble oxides undergoes the process of hydroxylation. The formation of hydroxyl groups depends on the physico-chemical conditions. On the surface of  $\text{SiO}_2$  there are surface hydroxyl groups (silanols) and, in some cases, water molecules inside the silica particles. The properties of such silica depend on the geometrical structure of pores and on the chemical properties of the silica surface [4, 5].

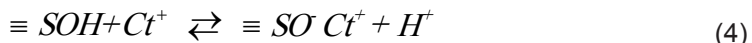
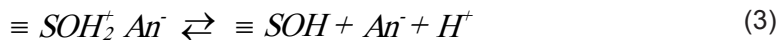
The skeleton of silica gel consists of spherical particles joined at points of contact. The pores are voids between the particles with different degree of packing. The size of the particles determines the size of the specific surface, and the density of packing determines the volume of pores and their radii. The silanol groups ( $\text{Si} \equiv -\text{OH}$ ) present on the silica surface are formed by two main processes. Such groups are formed in the synthesis of silica, and more specifically in the polymerisation of  $\text{Si(OH)}_4$ . The supersaturated solution of silicic acid enters the polymerised form, which is next transformed into spherical colloidal particles containing surface groups  $\text{Si} \equiv -\text{OH}$ . During drying, hydrogel is transformed into the final product – xerogel, which contains some or most of the surface silanol groups. The  $\text{Si} \equiv -\text{OH}$  surface groups can also form in water or in an aqueous solution as a result of the rehydroxylation of silica free from the hydroxyl groups. The surface silicon atoms tend to form a tetrahedron configuration and in aqueous solutions their free bonds are saturable with hydroxyl groups [4, 5].

The electric charge on the surface of the metal oxide in an aqueous electrolyte solution is formed due to a reaction of the surface hydroxyl groups with ions from the solution. The reaction of these groups with the  $H^+$  or  $OH^-$  ions in an electrolyte solution leads to the formation of groups endowed with positive or negative charge. These reactions are set out in the theory of *site binding* as ionisation reactions of the surface hydroxyl groups [6–10].



where  $\equiv S$  is the surface.

In view of the fact that  $H^+$  ions create a charge on the surface of oxides, in these systems they are considered the potential-forming ions. An important role in the formation of charge for such systems play the ions in a carrier electrolyte. Early classic theories of the "electrical double layer" (*edl*) initially assumed that these ions are subject to non-specific adsorption, while in more complex models of the *edl*, ions of the carrier electrolyte can also undergo the specific adsorption. According to the theory of "site binding", characteristic of these systems, carrier electrolyte ions react with the oxide surface hydroxyl groups to form a complex bond, e.g. for the metal oxide with a hypothetical electrolyte  $AnCt$  acting as a carrier electrolyte. The following complex reactions may occur on the surface of oxide:



where  $Ct^+$  represents a cation and  $An^-$  anion of the carrier electrolyte.

The mechanism of the charge formation on the surface of metal oxides in electrolyte solutions based on the reactions of 1–4 allows for recognition of the – observed in these systems – increase in charge density and the simultaneous decrease in Zeta potential with increasing concentration of the electrolyte [6, 11–14]. The reactions of ionisation and complexation of surface hydroxyl groups can be described with the following thermodynamic equilibrium constants:

$$K_{a1} = \frac{[H^+] [\equiv SOH]}{[\equiv SOH_2^+]} \frac{\gamma_H \gamma_0}{\gamma_+} \cdot \exp\left(\frac{-e\Psi_0}{k \cdot T}\right) \quad (5)$$

$$K_{a2} = \frac{[H^+] [\equiv SO^-]}{[\equiv SOH]} \frac{\gamma_H \gamma_-}{\gamma_0} \cdot \exp\left(\frac{-e\Psi_0}{k \cdot T}\right) \quad (6)$$

$$K_{An} = \frac{[H^+][An^-][\equiv SOH]}{\equiv SOH_2^+ An^-} \frac{\gamma_H \gamma_0 \gamma_{An}}{\gamma_{\pm}} \cdot \exp\left(\frac{-e(\Psi_0 - \Psi_{\beta})}{k \cdot T}\right) \quad (7)$$

$$K_{Ct} = \frac{[H^+][\equiv SO^- Ct^+]}{[\equiv SOH][Ct^+]} \frac{\gamma_H \gamma_{\pm}}{\gamma_0 \gamma_{Ct}} \cdot \exp\left(\frac{-e(\Psi_0 - \Psi_{\beta})}{k \cdot T}\right) \quad (8)$$

were:

- $K_{a1}$  – the equilibrium dissociation constant for the  $\equiv SOH_2^+$  group,
- $K_{a2}$  – the equilibrium constant for the formation of the  $\equiv SO^-$  surface groups,
- $\Psi_0$  – surface potential,
- $T$  – temperature,
- $k$  – Boltzmann constant,
- $e$  – elementary charge (electron),
- $\gamma_H$  – the activity coefficient of  $H^+$  ions,
- $\gamma_0$  – the activity coefficient of  $\equiv SOH$  groups,
- $\gamma_+$  – the activity coefficient of  $\equiv SOH_2^+$  group,
- $\gamma_-$  – the activity coefficient of  $\equiv SO^-$  groups,
- $K_{An}$  – the equilibrium constant for the reaction of anion complexation,
- $K_{Ct}$  – the equilibrium constant for the reaction of the cation complexation,
- $\Psi_{\beta}$  – the potential of inner Helmholtz plane,
- $\gamma_{An}$  – the activity coefficient of anions  $An^-$ ,
- $\gamma_{Ct}$  – the activity coefficient of cations  $Ct^+$ ,
- $\gamma_{\pm}$  – the activity coefficient  $\equiv SOH_2^+ An^-$  groups,
- $\gamma_{\mp}$  – the activity coefficient  $\equiv SO^- Ct^+$  groups.

The equilibrium constants of the ionisation and complexation reactions are not only the parameters characterising the electrical double layer at the metal oxide – aqueous electrolyte solution interface, but also allow us to calculate the charge and potential distribution within the *edl*. Our knowledge of the distribution of the electric potential and electric charge within the *edl* is one of the important elements in the theory of the stability of dispersed systems. Moreover, these constants, as well as the complexation constants in solution, allow us to calculate the concentration of each surface compound, and in the case of ions adsorption – the ion partition coefficient between the solution and solid phase.

The surface charge density is proportional to an algebraic sum of the concentration of the ionised groups and complexes:

$$\sigma_0 = B_N \{ [ \equiv SOH_2^+ ] + [ \equiv SOH_2^+ An^- ] - [ \equiv SO^- ] - [ \equiv SO^- Ct^+ ] \} \quad (9)$$

where  $Ct^+$  represents a cation and  $An^-$  an anion of the carrier electrolyte.

The concentration of the potential-forming ions at which the surface charge density is zero is called "point of zero-charge" ( $pzc$ ). In the case of metal oxide, the potential-forming ions are  $H^+$  ions. Therefore, this point is related with a pH scale and is referred to as  $pH_{pzc}$ . In  $pH_{pzc}$  the total charge density is zero, which means that the concentration of positively charged groups is equal to the concentration of negatively charged groups:

$$\sigma_0 = 0 \Rightarrow [ \equiv SOH_2^+ ] + [ \equiv SOH_2^+ An^- ] = [ \equiv SO^- ] + [ \equiv SO^- Ct^+ ] \quad (10)$$

The carrier electrolyte ions involved in reactions 3 and 4 occupy positions in the "inner Helmholtz plane" (*IHP*) and are labelled with the  $\beta$  symbol. This level is attributed to the specifically adsorbed ions  $\sigma_\beta$  and potential  $\psi_\beta$ . The density of charge adsorbed by the *IHP* in a "metal oxide - electrolyte solution" system (1:1) is equal to:

$$\sigma_\beta = B_N \{ [ \equiv SO^- Ct^+ ] - [ \equiv SOH_2^+ An^- ] \} \quad (11)$$

To estimate the density of ions adsorbed by the *IHP* it is assumed that ion density in the carrier electrolyte located in the *edl* diffusion layer corresponds to the electric charge in the diffusion layer and can be calculated from the Gouy-Chapman equation, knowing the value of Zeta potential. Thus, the density of ions forming surface complexes is equal to:

$$\sigma_{\beta,An(Ct)} = \sigma_{An(ct)} - \sigma_d \quad (12)$$

Part of the surface charge derived from the ionised groups is compensated in the diffusion part of the electrical double layer. The diffusion part of the layer accumulates ions which are adsorbed by an electrostatic interaction. The adsorption of these ions is called non-specific adsorption. The diffusion layer is characterised by the diffusion layer potential  $\psi_d$  and diffusion layer charge density  $\sigma_d$ . The charge density of the diffusion layer will be equal to:

$$\sigma_d = B_N \{ [ \equiv SO^- ] - [ \equiv SOH_2^+ ] \} \quad (13)$$

The relationship between surface potential and charge density for a symmetric electrolyte is expressed by the equation:

$$\sigma_d = \sqrt{8000 \epsilon \epsilon_0 c R T} \sinh \left( \frac{z e \psi_d}{k T} \right) \quad (14)$$

where:

$\psi_d$  – the potential of diffusion layer,  
 $T$  – temperature,  
 $k$  – Boltzmann constant,  
 $e$  – elementary charge (electron),  
 $z$  – valence ions of the carrier electrolyte,  
 $\epsilon$  – relative dielectric permittivity of the medium,  
 $\epsilon_0$  – dielectric permittivity of vacuum,  
 $R$  – gas constant,  
 $c$  – concentration of the electrolyte.

The potential of the diffusion layer of the electrical double layer  $edl$  can be determined from the measurements of *Zeta* potential, allowing for a distance between the slip plane (determining the value of *Zeta* potential) and the "outer Helmholtz plane" (*OHP*), with which the potential of the diffusion layer is associated.

To determine the value of the diffusion layer potential it is necessary to know the slip plane distance from the *OHP*. This distance is not determined in a consistent manner and – depending on the system – ranges from 0.4 nm to 2.0 nm. It depends, among others, on the porosity of the solid [15]. As stated above, ion concentration at which the *Zeta* potential is zero is called "isoelectric point". In the case of metal oxides, this point is also referred to the *pH* scale. At the *isoelectric point*, the charge density in the diffusion layer is equal to 0. This means that on the oxide surface the concentration of positively ionised groups is equal to the concentration of negatively ionised groups.

The *Zeta* potential of colloids with the liquid phase acting as a dispersed phase is usually determined by microelectrophoresis. Other electrokinetic phenomena are much less common in such cases [16–19].

The correct values of electrophoretic mobility (free from the so-called "side wall effect"), at the stationary level in zeta meters with a constant voltage, are obtained for a rectangular cell with a height-to-width ratio greater than 1:20. The hydroxyl groups on the surface of  $SiO_2$  in electrolyte solutions behave similarly to hydroxyl groups on the surface of metal oxides. The charge on the surface is formed by the reaction of surface hydroxyl groups (silanol groups) with the ions  $H^+$  or  $OH^-$  and by complexation reactions with ions of the carrier electrolyte.

To determine changes in the *Zeta* potential after certain time of gelation going on in the "soluble sodium silicate – ester hardener" system, a sample was taken and introduced to the carrier electrolyte. Before making the dispersion, the electrolyte solutions were filtered on a membrane filter with the pore diameter of 0.22  $\mu m$  to remove the insoluble impurities. Based on the results of the preliminary measurements, an optimum ratio of the "soluble sodium silicate – ester hardener" sample addition to the carrier electrolyte was determined. With this ratio, the signal recorded for the scattered laser light was optimal, and the measured values of *Zeta* potential were the same as at a higher dilution. After

preparation, the dispersed sample was subjected to the effect of ultrasounds and its *pH* value was measured. Since the systems studied were characterised by certain heterogeneity of the dispersed phase, the average *Zeta* potential distribution was calculated by averaging the individual distributions (summed channel by channel, and calculating the average of 3–5 measurements).

Preliminary measurements of the *Zeta* potential of the examined "soluble sodium silicate – ester hardener" samples revealed the presence of particles undergoing electrophoresis. The measurement results are shown in Figure 1.

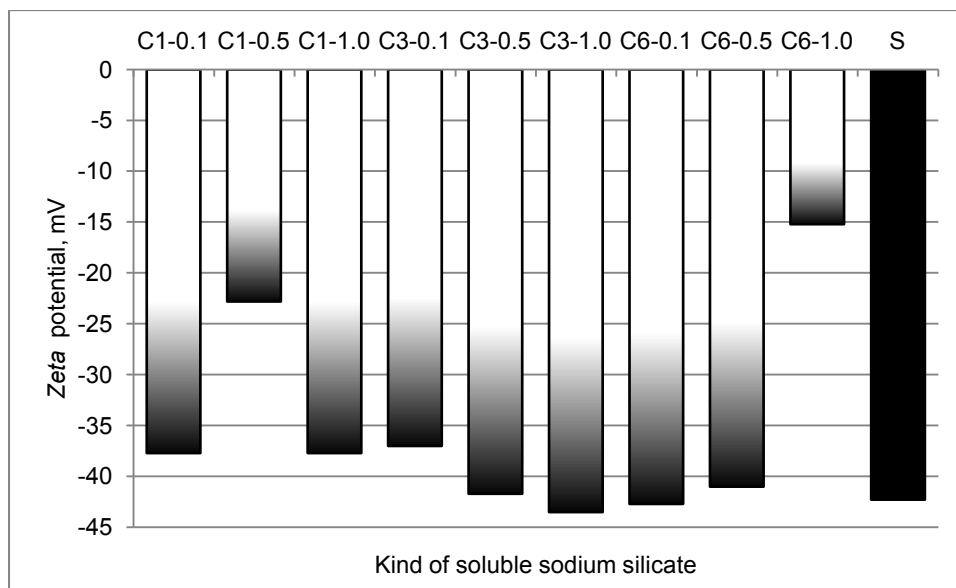


Fig. 1. *Zeta* potential of the investigated types of soluble sodium silicate

Rys. 1. Potencjał *Zeta* badanych rodzajów uwodnionego krzemianu sodu

The study of the kinetics of changes in the electrokinetic *Zeta* potential in function of the gelation time was carried out on the "soluble sodium silicate – hardener ester" gel samples taken after the gelation time of 20, 30, 40, 60, 80 and 100 min. Figures 2–19 show changes in the *Zeta* potential of gel samples obtained from the following soluble sodium silicates: C1-0.1, C1-0.5, C1-1.0, C3-0.1, C3-0.5, C3-1.0, C6-0.1, C6-0.5, C6-1.0, and from the chemically unmodified standard soluble silicates S. The *pH* values of dispersion samples obtained from the gel varied from  $pH \approx 11$  for the shortest gelation time to  $pH \approx 10.3$  obtained after 100 minutes of gelation. The *pH* values differed little for individual samples and had no significant effect on the *Zeta* potential values. Figures 20–25 show the value of the first maximum of electrophoretic signal intensity / on the surface of colloidal particles in the gelling system "chemically modified and unmodified soluble sodium silicate – ester hardener" gelling system and the corresponding *Zeta* potential values. Figures 26–31 show the value of the second maximum of electrophoretic signal intensity / on the surface of colloidal particles in the "chemically modified and unmodified soluble sodium silicate – ester hardener" gelling system and the corresponding *Zeta* potential values.

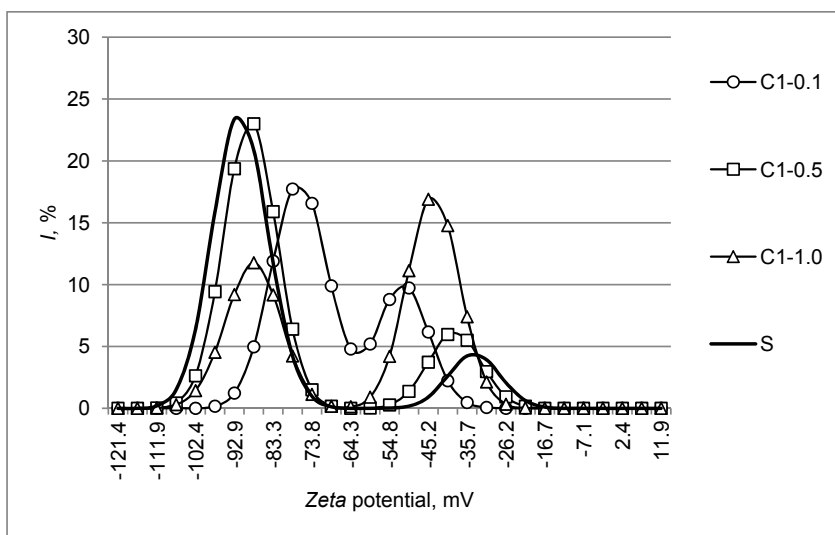


Fig. 2. Electrophoretic signal intensity  $I$  as a function of Zeta potential of colloidal particles formed after gelling for 20 minutes the "soluble sodium silicate of type C1 and S – ester hardener" system

Rys. 2. Intensywność sygnału elektroforetycznego  $I$  w funkcji potencjału Zeta cząstek koloidalnych powstających po czasie żelowania 20 minut układu „uwodniony krzemian typu C1 i S – utwardzacz estrowy”

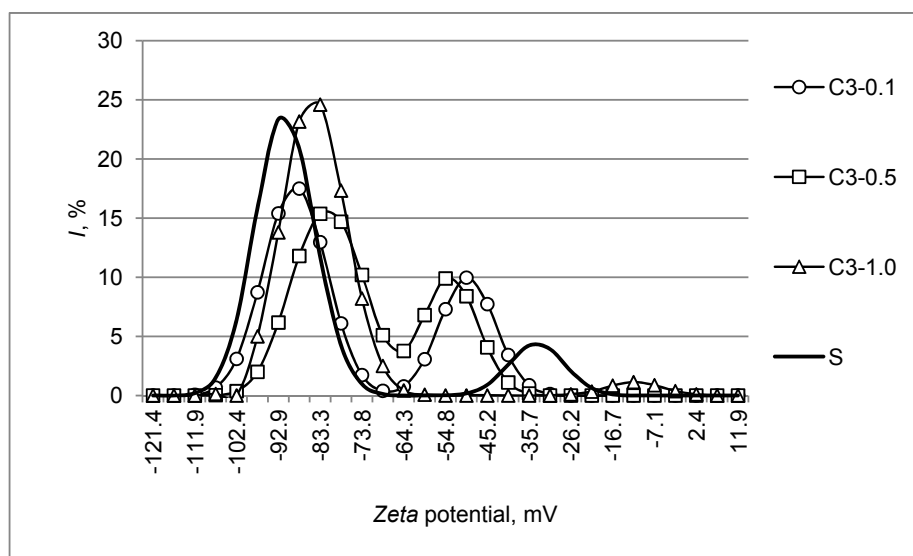


Fig. 3. Electrophoretic signal intensity  $I$  as a function of Zeta potential of colloidal particles formed after gelling for 20 minutes the "soluble sodium silicate of type C3 and S – ester hardener" system

Rys. 3. Intensywność sygnału elektroforetycznego  $I$  w funkcji potencjału Zeta cząstek koloidalnych powstających po czasie żelowania 20 minut układu „uwodniony krzemian typu C3 i S – utwardzacz estrowy”

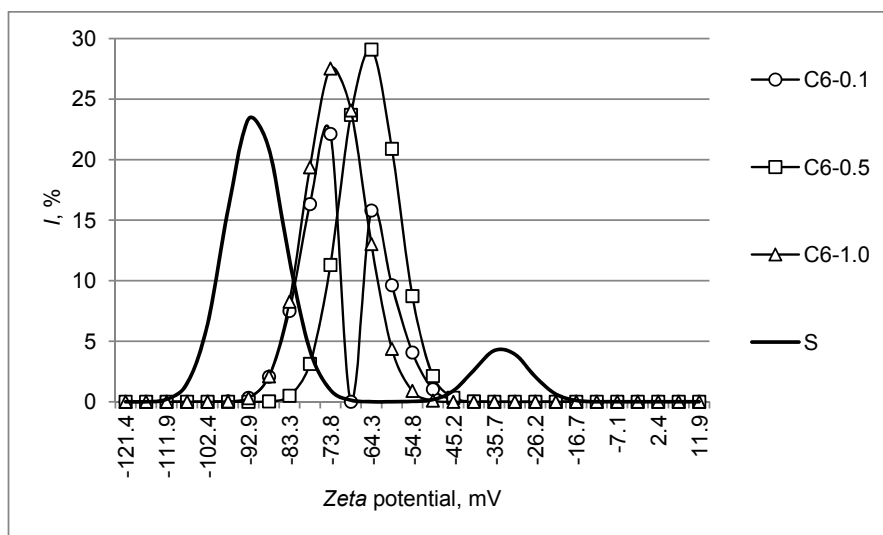


Fig. 4. Electrophoretic signal intensity  $I$  as a function of Zeta potential of colloidal particles formed after gelling for 20 minutes the "soluble sodium silicate of type C6 and S – ester hardener" system

Rys. 4. Intensywność sygnału elektroforetycznego  $I$  w funkcji potencjału Zeta cząstek koloidalnych powstały po czasie żelowania 20 minut układu „uwodniony krzemian typu C6 i S – utwardzacz estrowy”

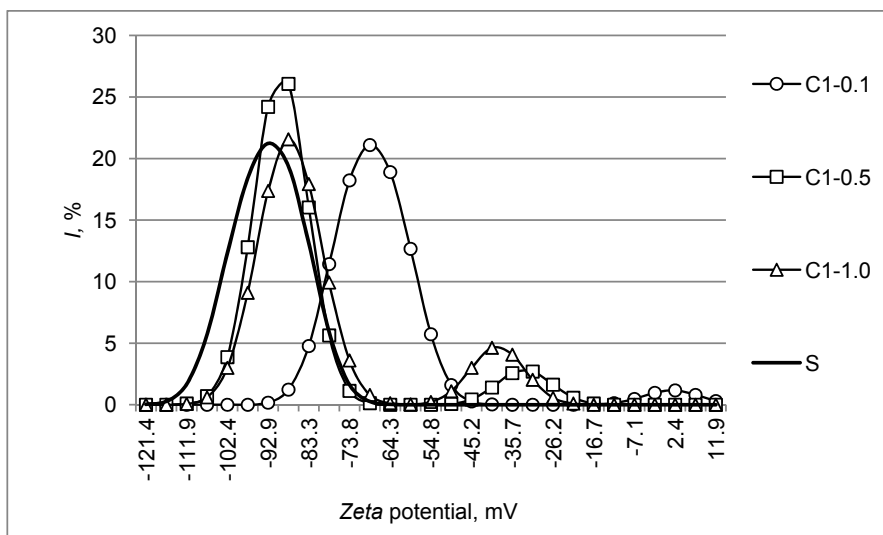


Fig. 5. Electrophoretic signal intensity  $I$  as a function of Zeta potential of colloidal particles formed after gelling for 30 minutes the "soluble sodium silicate of type C1 and S – ester hardener" system

Rys. 5. Intensywność sygnału elektroforetycznego  $I$  w funkcji potencjału Zeta cząstek koloidalnych powstały po czasie żelowania 30 minut układu „uwodniony krzemian typu C1 i S – utwardzacz estrowy”

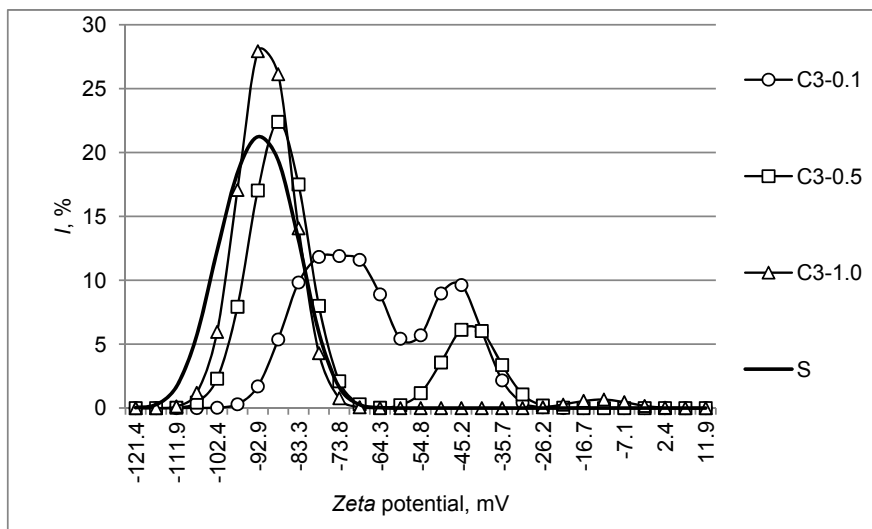


Fig. 6. Electrophoretic signal intensity  $I$  as a function of Zeta potential of colloidal particles formed after gelling for 30 minutes the "soluble sodium silicate of type C3 and S – ester hardener" system

Rys. 6. Intensywność sygnału elektroforetycznego  $I$  w funkcji potencjału Zeta cząstek koloidalnych powstających po czasie żelowania 30 minut układu „uwodniony krzemian typu C3 i S – utwardzacz estrowy”

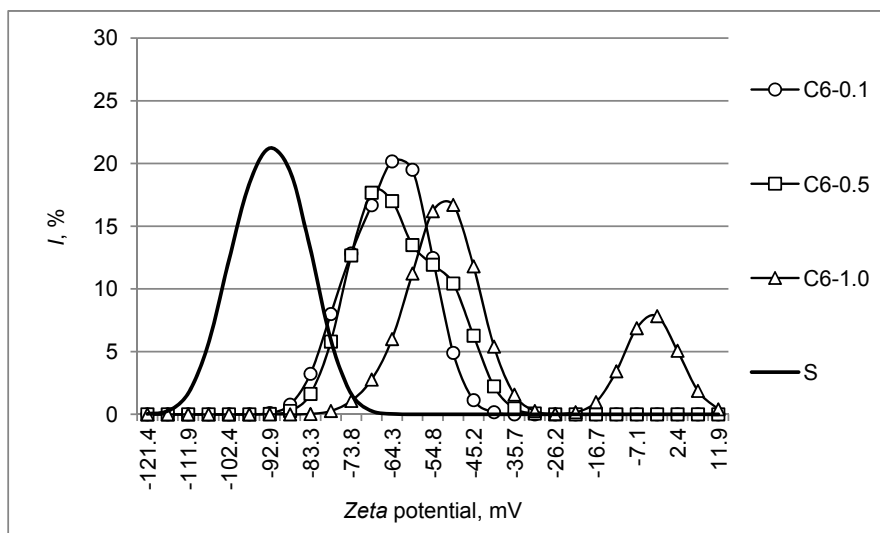


Fig. 7. Electrophoretic signal intensity  $I$  as a function of Zeta potential of colloidal particles formed after gelling for 30 minutes of the "soluble sodium silicate of type C6 and S – ester hardener" system

Rys. 7. Intensywność sygnału elektroforetycznego  $I$  w funkcji potencjału Zeta cząstek koloidalnych powstających po czasie żelowania 30 minut układu „uwodniony krzemian typu C6 i S – utwardzacz estrowy”

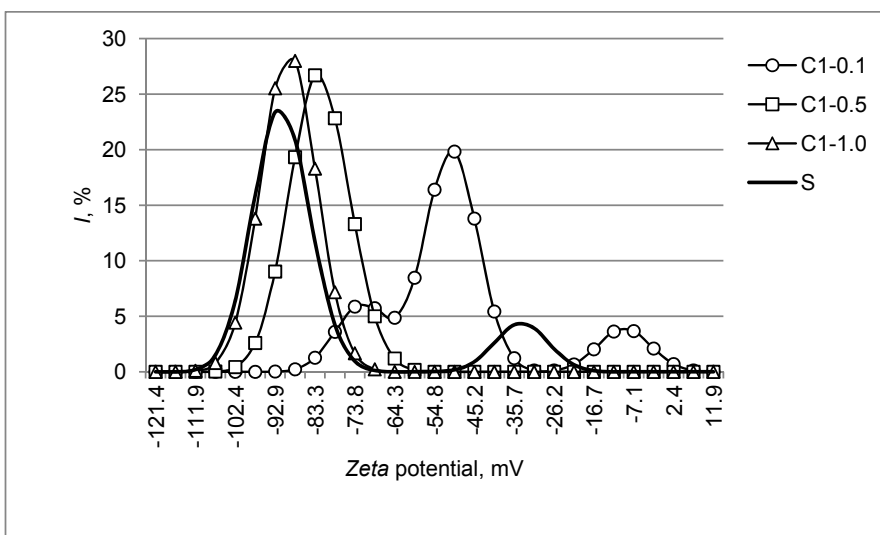


Fig. 8. Electrophoretic signal intensity  $I$  as a function of Zeta potential of colloidal particles formed after gelling for 40 minutes the "soluble sodium silicate of type C1 and S – ester hardener" system

Rys. 8. Intensywność sygnału elektroforetycznego  $I$  w funkcji potencjału Zeta cząstek koloidalnych powstały po czasie żelowania 40 minut układu „uwodniony krzemian typu C1 i S – utwardzacz estrowy”

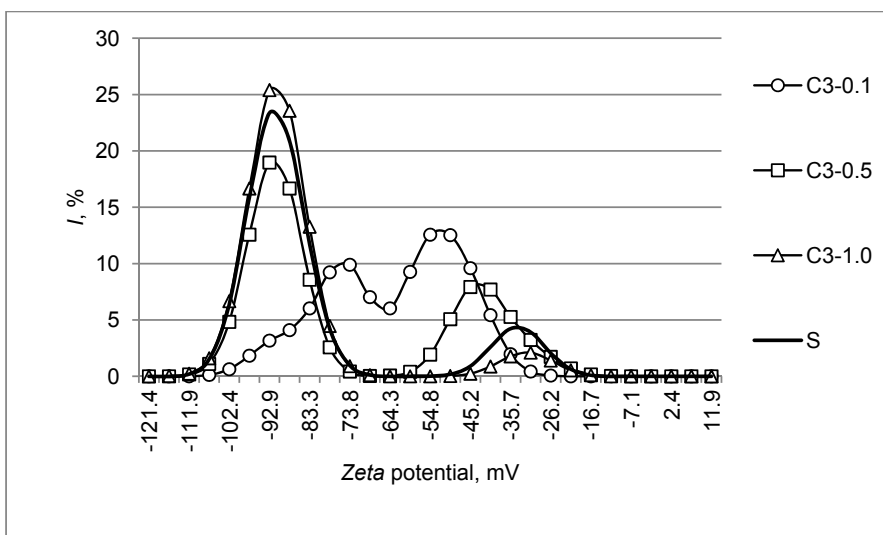


Fig. 9. Electrophoretic signal intensity  $I$  as a function of Zeta potential of colloidal particles formed after gelling for 40 minutes the "soluble sodium silicate of type C3 and S – ester hardener" system

Rys. 9. Intensywność sygnału elektroforetycznego  $I$  w funkcji potencjału Zeta cząstek koloidalnych powstały po czasie żelowania 40 minut układu „uwodniony krzemian typu C3 i S – utwardzacz estrowy”

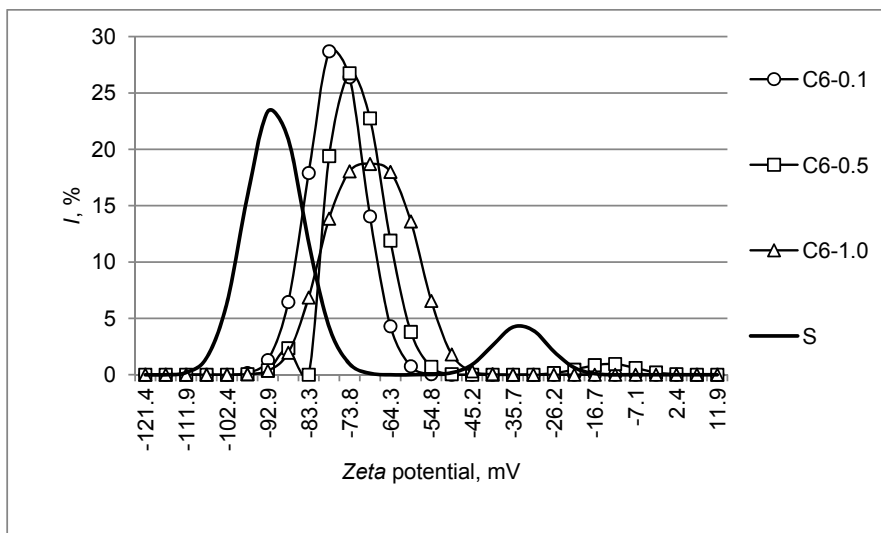


Fig. 10. Electrophoretic signal intensity  $I$  as a function of Zeta potential of colloidal particles formed after gelling for 40 minutes the "soluble sodium silicate of type C6 and S – ester hardener" system

Rys. 10. Intensywność sygnału elektroforetycznego  $I$  w funkcji potencjału Zeta cząstek koloidalnych powstających po czasie żelowania 40 minut układu „uwodniony krzemian typu C6 i S – utwardzacz estrowy”

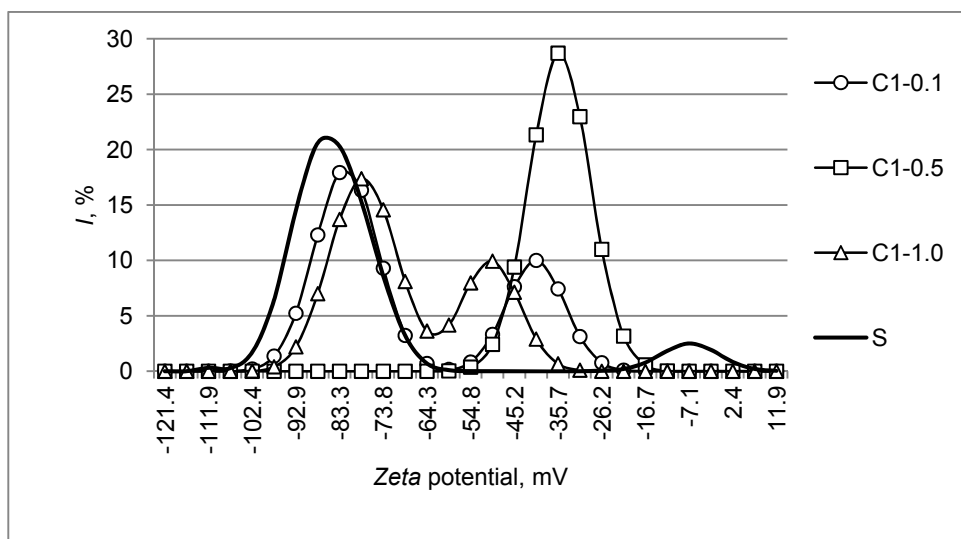


Fig. 11. Electrophoretic signal intensity  $I$  as a function of Zeta potential of colloidal particles formed after gelling for 60 minutes the "soluble sodium silicate of type C1 and S – ester hardener" system

Rys. 11. Intensywność sygnału elektroforetycznego  $I$  w funkcji potencjału Zeta cząstek koloidalnych powstających po czasie żelowania 60 minut układu „uwodniony krzemian typu C1 i S – utwardzacz estrowy”

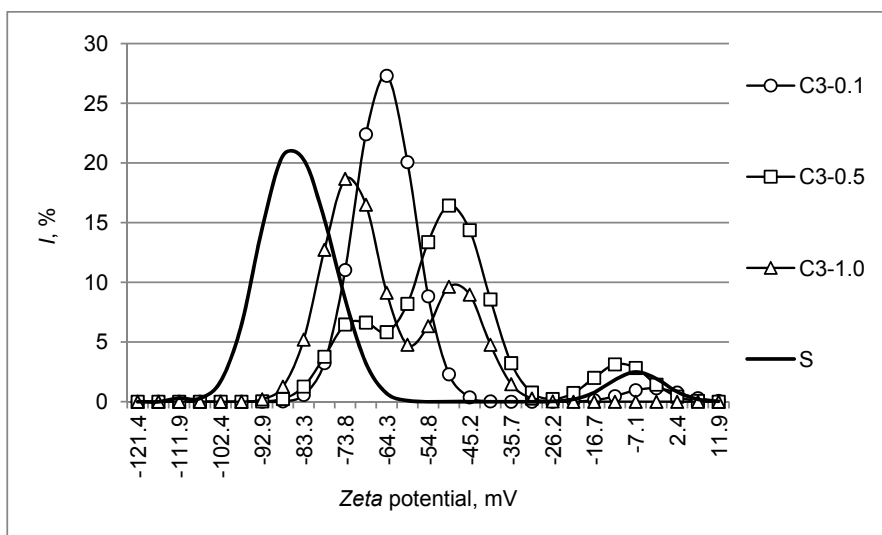


Fig. 12. Electrophoretic signal intensity  $I$  as a function of Zeta potential of colloidal particles formed after gelling for 60 minutes the "soluble sodium silicate of type C3 and S – ester hardener" system

Rys. 12. Intensywność sygnału elektroforetycznego  $I$  w funkcji potencjału Zeta cząstek koloidalnych powstały po czasie żelowania 60 minut układu „uwodniony krzemian typu C3 i S – utwardzacz estrowy”

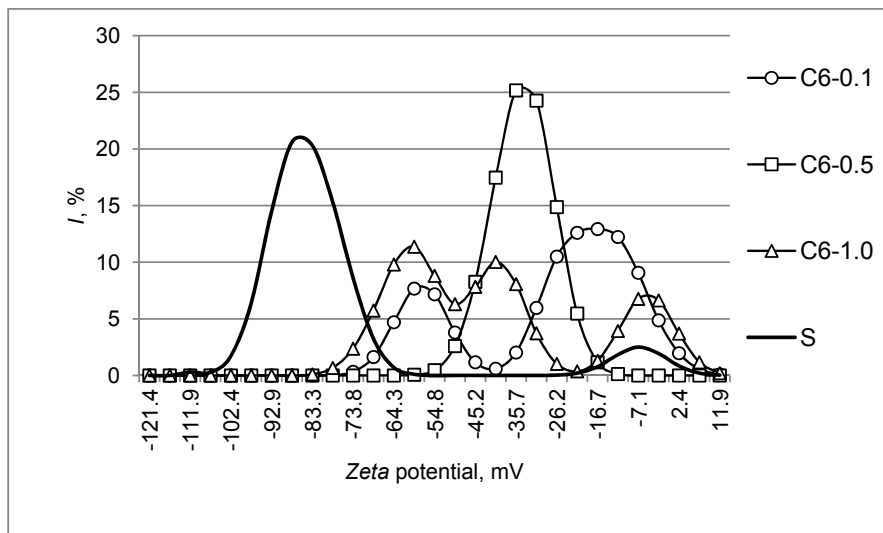


Fig. 13. Electrophoretic signal intensity  $I$  as a function of Zeta potential of colloidal particles formed after gelling for 60 minutes the "soluble sodium silicate of type C6 and S – ester hardener" system

Rys. 13. Intensywność sygnału elektroforetycznego  $I$  w funkcji potencjału Zeta cząstek koloidalnych powstały po czasie żelowania 60 minut układu „uwodniony krzemian typu C6 i S – utwardzacz estrowy”

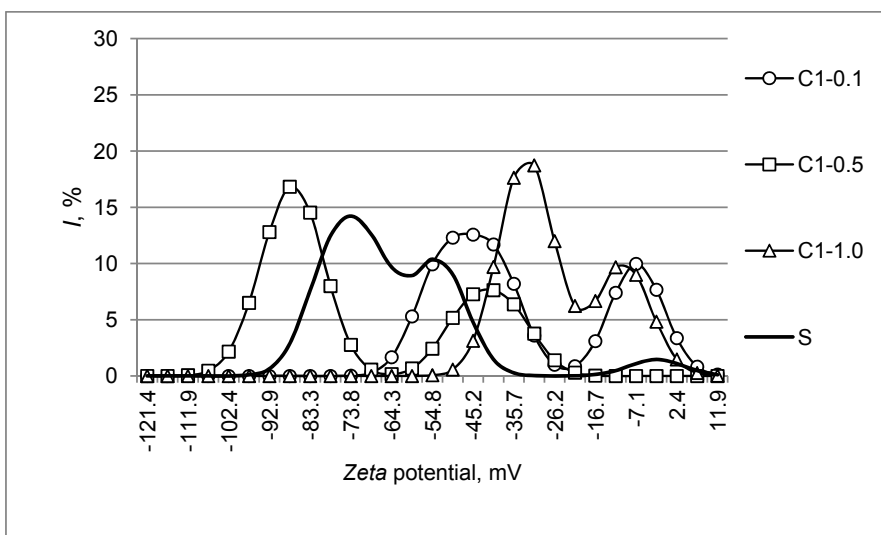


Fig. 14. Electrophoretic signal intensity  $I$  as a function of Zeta potential of colloidal particles formed after gelling for 80 minutes the "soluble sodium silicate of type C1 and S – ester hardener" system

Rys. 14. Intensywność sygnału elektroforetycznego  $I$  w funkcji potencjału Zeta cząstek koloidalnych powstających po czasie żelowania 80 minut układu „uwodniony krzemian typu C1 i S – utwardzacz estrowy”

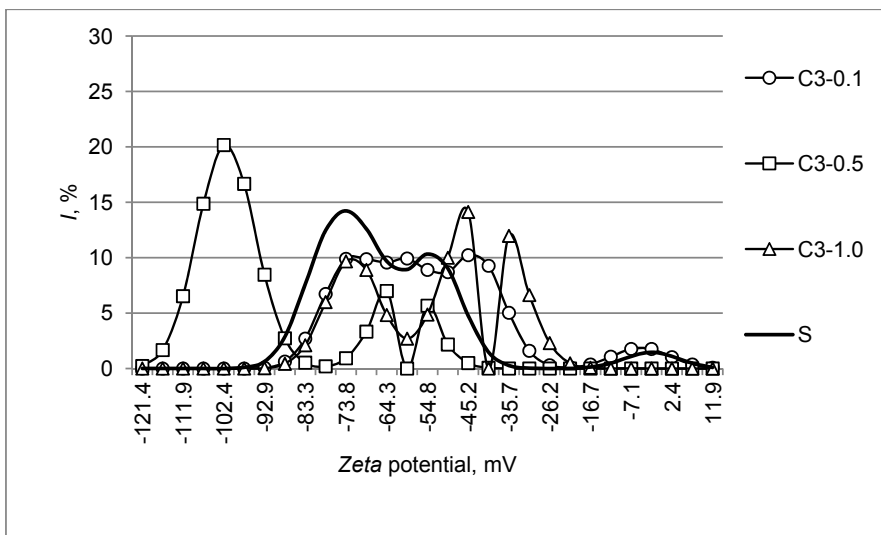


Fig. 15. Electrophoretic signal intensity  $I$  as a function of Zeta potential of colloidal particles formed after 80 minutes the "soluble sodium silicate of type C3 and S – ester hardener" system

Rys. 15. Intensywność sygnału elektroforetycznego  $I$  w funkcji potencjału Zeta cząstek koloidalnych powstających po czasie żelowania 80 minut układu „uwodniony krzemian typu C3 i S – utwardzacz estrowy”

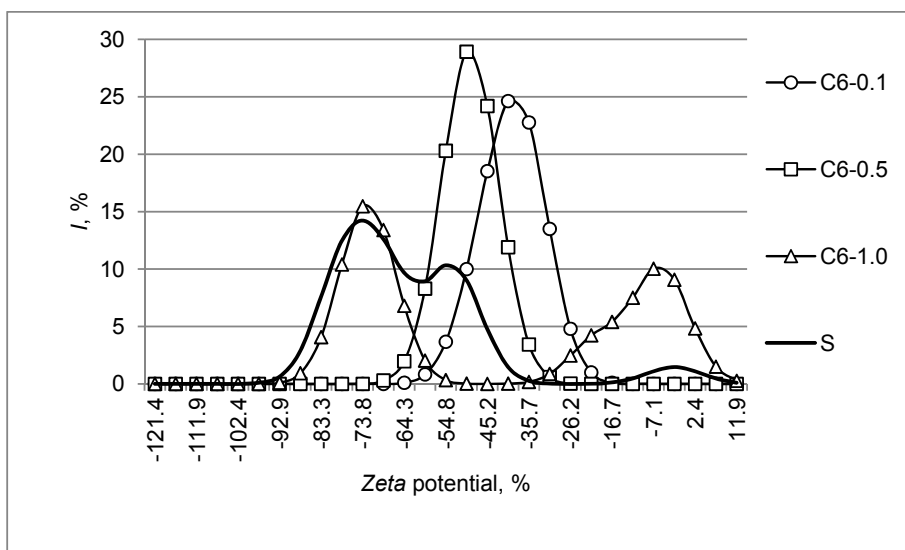


Fig. 16. Electrophoretic signal intensity  $I$  as a function of Zeta potential of colloidal particles formed after gelling for 80 minutes the "soluble sodium silicate of type C6 and S – ester hardener" system

Rys. 16. Intensywność sygnału elektroforetycznego  $I$  w funkcji potencjału Zeta cząstek koloidalnych powstały po czasie żelowania 80 minut układu „uwodniony krzemian typu C6 i S – utwardzacz estrowy”

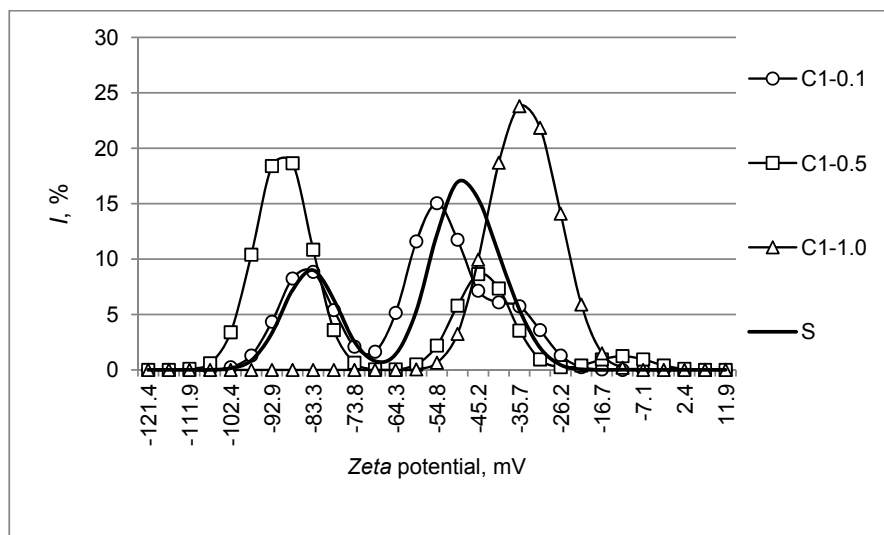


Fig. 17. Electrophoretic signal intensity  $I$  as a function of Zeta potential of colloidal particles formed after gelling for 100 minutes the "soluble sodium silicate of type C1 and S – ester hardener" system

Rys. 17. Intensywność sygnału elektroforetycznego  $I$  w funkcji potencjału Zeta cząstek koloidalnych powstały po czasie żelowania 100 minut układu „uwodniony krzemian typu C1 i S – utwardzacz estrowy”

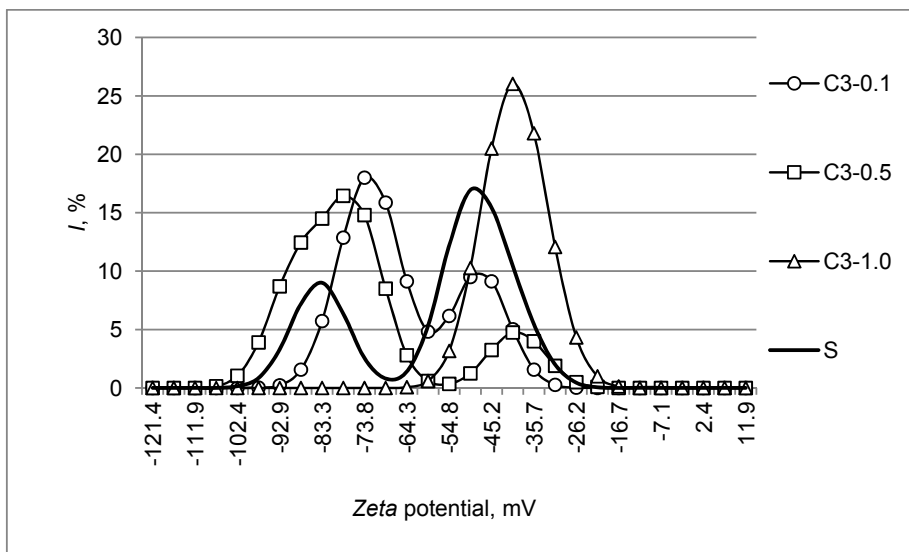


Fig. 18. Electrophoretic signal intensity  $I$  as a function of Zeta potential of colloidal particles formed after gelling for 100 minutes the "soluble sodium silicate of type C3 and S – ester hardener" system

Rys. 18. Intensywność sygnału elektroforetycznego  $I$  w funkcji potencjału Zeta cząstek koloidalnych powstały po czasie żelowania 100 minut układu „uwodniony krzemian typu C3 i S – utwardzacz estrowy”

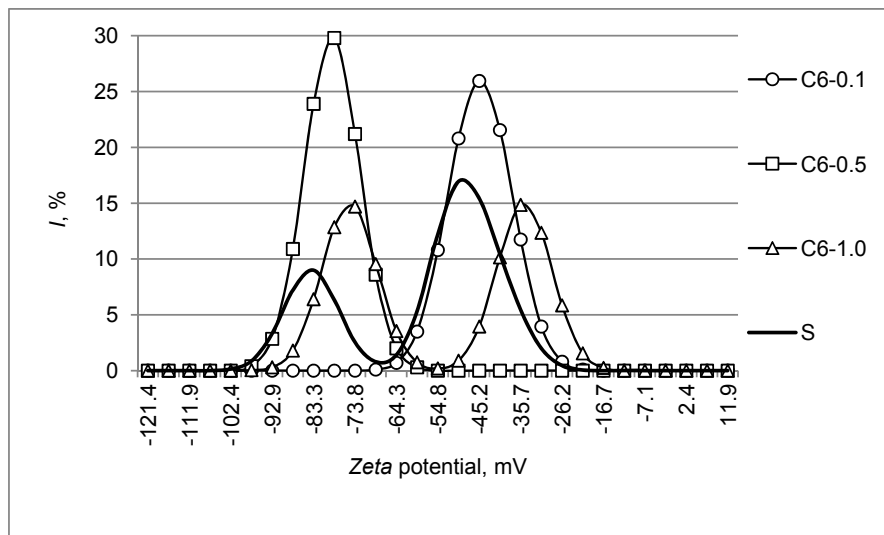


Fig. 19. Electrophoretic signal intensity  $I$  as a function of Zeta potential of colloidal particles formed after gelling for 100 minutes the "soluble sodium silicate of type C6 and S – ester hardener" system

Rys. 19. Intensywność sygnału elektroforetycznego  $I$  w funkcji potencjału Zeta cząstek koloidalnych powstały po czasie żelowania 100 minut układu „uwodniony krzemian typu C6 i S – utwardzacz estrowy”

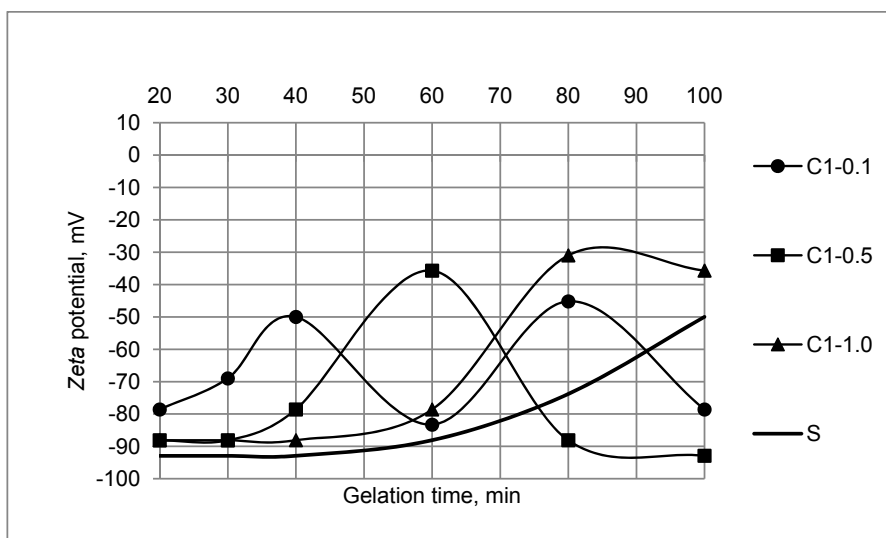


Fig. 20. The first maximum of electrophoretic signal intensity I and corresponding Zeta potential of colloidal particles formed after gelling the "soluble sodium silicate type C1-0.1, C1-0.5, C1-1.0 and S – ester hardener" system

Rys. 20. Pierwsze maksimum intensywności sygnału elektroforetycznego I oraz odpowiadający mu potencjał Zeta cząstek koloidalnych powstających w żelującym układzie „uwodniony krzemian sodu rodzaju C1-0.1, C1-0.5, C1-1.0 i S – utwardzacz estrowy”

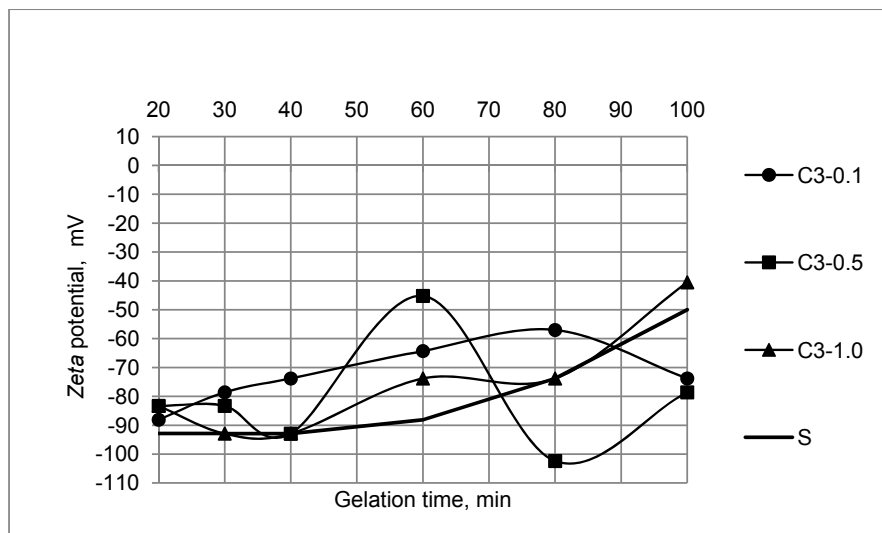


Fig. 21. The first maximum of electrophoretic signal intensity I and corresponding Zeta potential of colloidal particles formed after gelling the "soluble sodium silicate type C3-0.1, C3-0.5, C3-1.0 and S – ester hardener" system

Rys. 21. Pierwsze maksimum intensywności sygnału elektroforetycznego I oraz odpowiadający mu potencjał Zeta cząstek koloidalnych powstających w żelującym układzie „uwodniony krzemian sodu rodzaju C3-0.1, C3-0.5, C3-1.0 i S – utwardzacz estrowy”

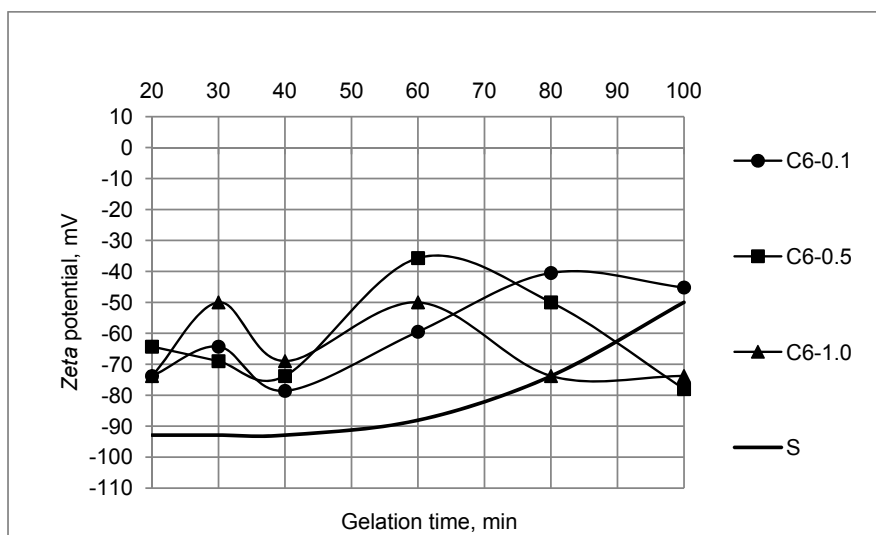


Fig. 22. The first maximum of electrophoretic signal intensity I and corresponding Zeta potential of colloidal particles formed after gelling the "soluble sodium silicate type C6-0.1, C6-0.5, C6-1.0 and S – ester hardener" system

Rys. 22. Pierwsze maksimum intensywności sygnału elektroforetycznego I oraz odpowiadający mu potencjał Zeta cząstek koloidalnych powstających w żelującym układzie „uwodniony krzemian sodu rodzaju C6-0.1, C6-0.5, C6-1.0 i S – utwardzacz estrowy”

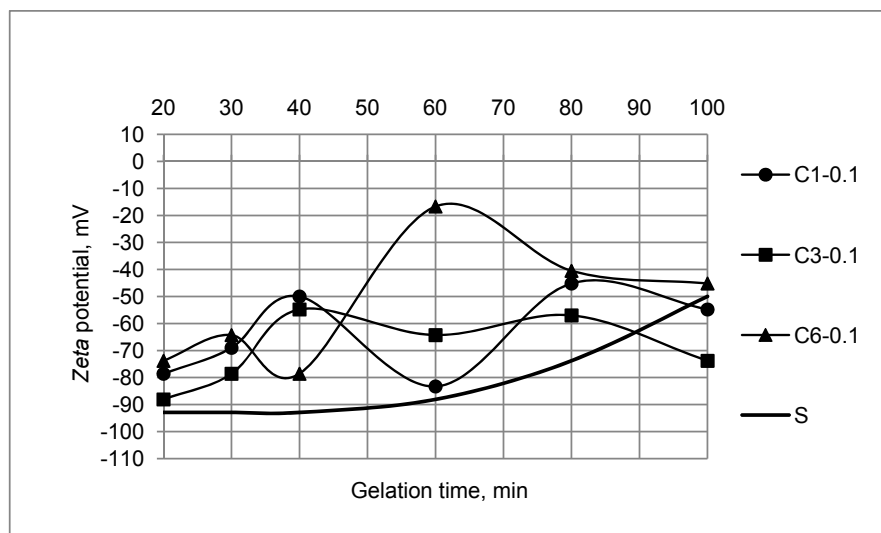


Fig. 23. The first maximum of electrophoretic signal intensity I and corresponding Zeta potential of colloidal particles formed after gelling the "soluble sodium silicate type C1-0.1, C3-0.1, C6-0.1 and S – ester hardener" system

Rys. 23. Pierwsze maksimum intensywności sygnału elektroforetycznego I oraz odpowiadający mu potencjał Zeta cząstek koloidalnych powstających w żelującym układzie „uwodniony krzemian sodu rodzaju C1-0.1, C3-0.1, C6-0.1 i S – utwardzacz estrowy”

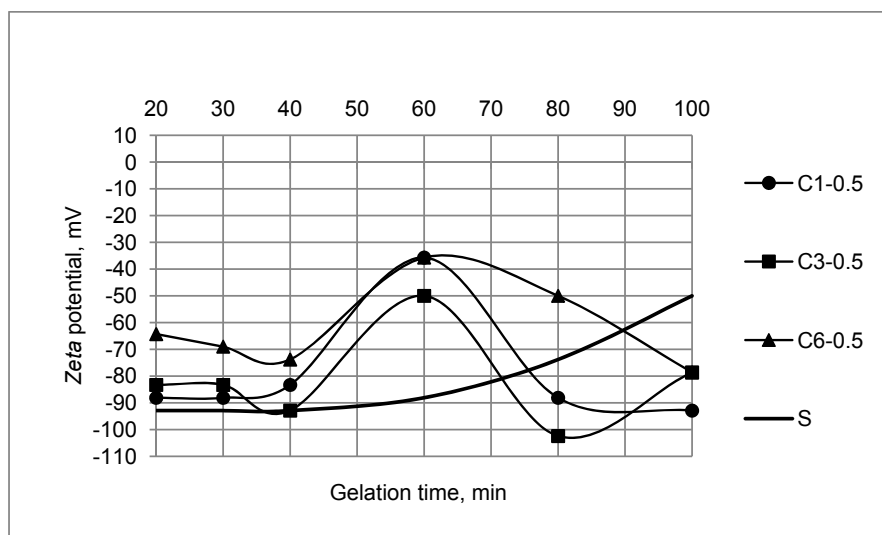


Fig. 24. The first maximum of electrophoretic signal intensity I and corresponding Zeta potential of colloidal particles formed after gelling the "soluble sodium silicate type C1-0.5, C3-0.5, C6-0.5 and S – ester hardener" system

Rys. 24. Pierwsze maksimum intensywności sygnału elektroforetycznego I oraz odpowiadający mu potencjał Zeta cząstek koloidalnych powstających w żelującym układzie „uwodniony krzemian sodu rodzaju C1-0,5, C3-0,5, C6-0,5 i S – utwardzacz estrowy”

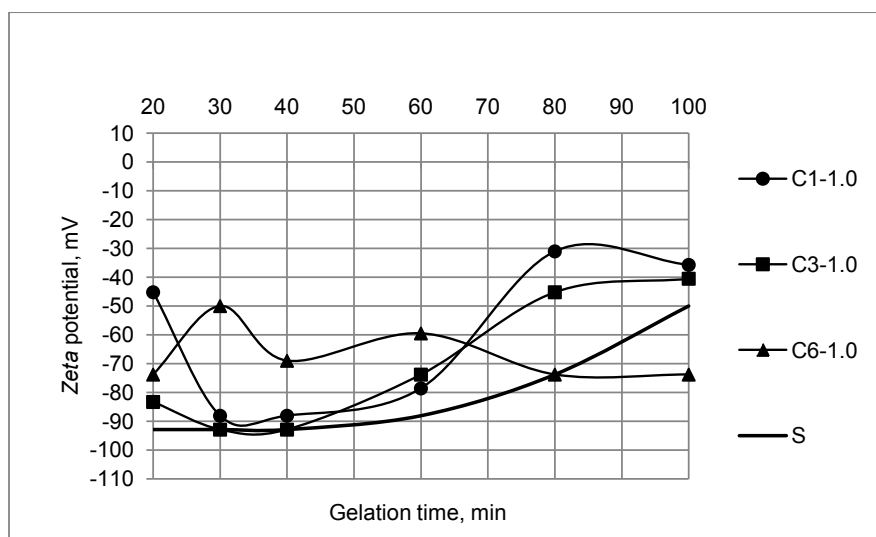


Fig. 25. The first maximum of electrophoretic signal intensity I and corresponding Zeta potential of colloidal particles formed after gelling the "soluble sodium silicate type C1-1.0, C3-1.0, C6-1.0 and S – ester hardener" system

Rys. 25. Pierwsze maksimum intensywności sygnału elektroforetycznego I oraz odpowiadający mu potencjał Zeta cząstek koloidalnych powstających w żelującym układzie „uwodniony krzemian sodu rodzaju C1-1,0, C3-1,0, C6-1,0 i S – utwardzacz estrowy”

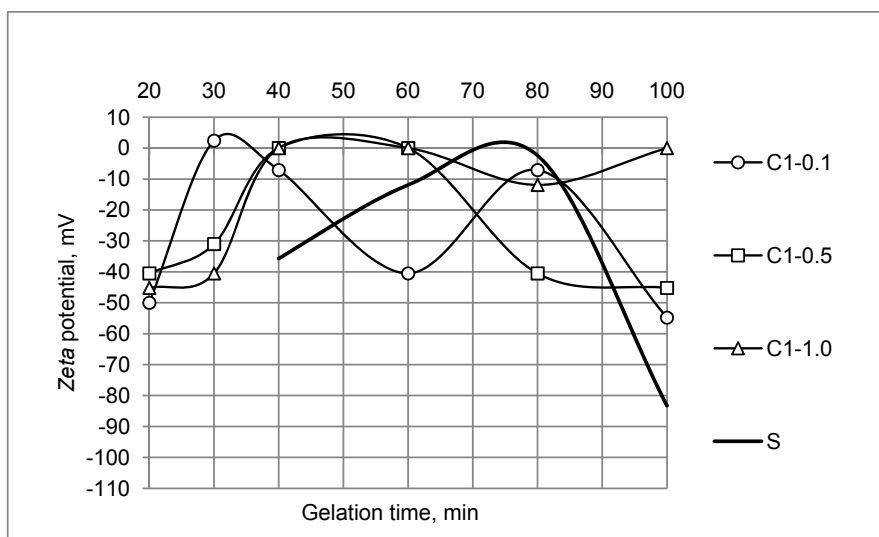


Fig. 26. The second maximum of electrophoretic signal intensity I and corresponding Zeta potential of colloidal particles formed after gelling the "soluble sodium silicate type C1-0.1, C1-0.5, C1-1.0 and S – ester hardener" system

Rys. 26. Drugie maksimum intensywności sygnału elektroforetycznego I oraz odpowiadający mu potencjał Zeta cząstek koloidalnych powstających w żelującym układzie „uwodniony krzemian sodu rodzaju C1-0.1, C1-0.5, C1-1.0 i S – utwardzacz estrowy”

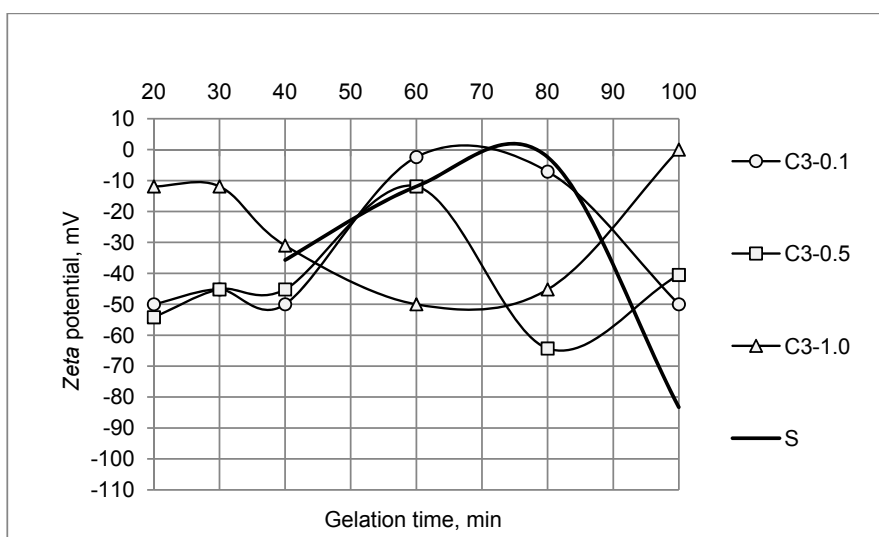


Fig. 27. The second maximum of electrophoretic signal intensity I and corresponding Zeta potential of colloidal particles formed after gelling the "soluble sodium silicate type C3-0.1, C3-0.5, C3-1.0 and S – ester hardener" system

Rys. 27. Drugie maksimum intensywności sygnału elektroforetycznego I oraz odpowiadający mu potencjał Zeta cząstek koloidalnych powstających w żelującym układzie „uwodniony krzemian sodu rodzaju C3-0.1, C3-0.5, C3-1.0 i S – utwardzacz estrowy”

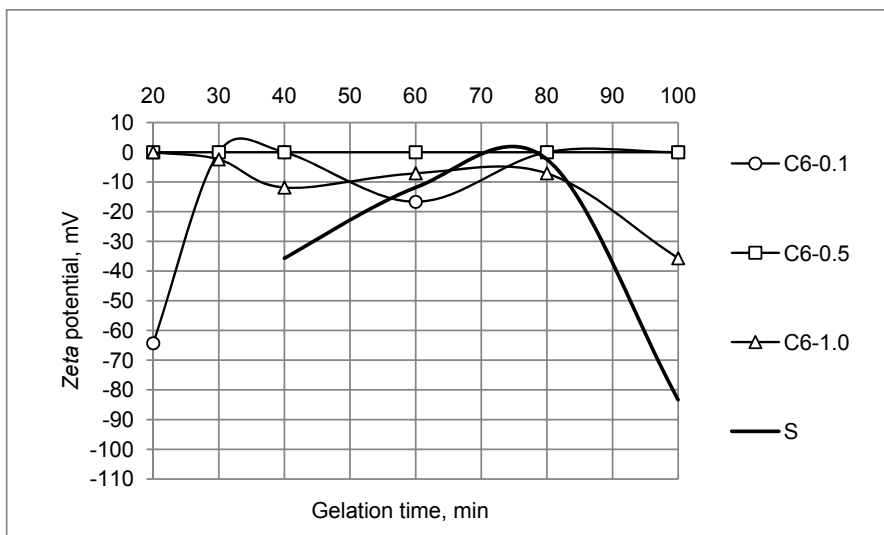


Fig. 28. The second maximum of electrophoretic signal intensity I and corresponding Zeta potential of colloidal particles formed after gelling the "soluble sodium silicate type C6-0.1, C6-0.5, C6-1.0 and S – ester hardener" system

Rys. 28. Drugie maksimum intensywności sygnału elektroforetycznego I oraz odpowiadający mu potencjał Zeta cząstek koloidalnych powstających w żelującym układzie „uwodniony krzemian sodu rodzaju C6-0.1, C6-0.5, C6-1.0 i S – utwardzacz estrowy”

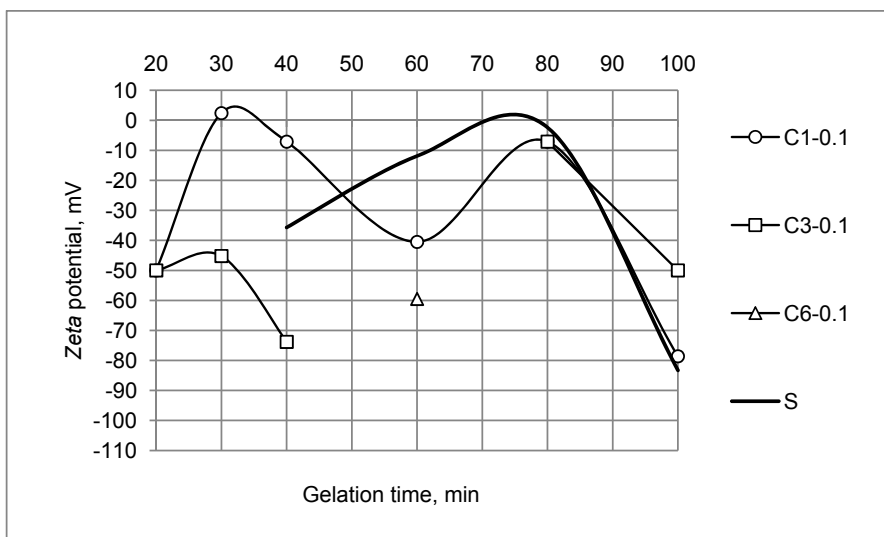


Fig. 29. The second maximum of electrophoretic signal intensity I and corresponding Zeta potential of colloidal particles formed after gelling the "soluble sodium silicate type C1-0.1, C3-0.1, C6-0.10 and S – ester hardener" system

Rys. 29. Drugie maksimum intensywności sygnału elektroforetycznego I oraz odpowiadający mu potencjał Zeta cząstek koloidalnych powstających w żelującym układzie „uwodniony krzemian sodu rodzaju C1-0.1, C3-0.1, C6-0.10 and S – ester hardener”

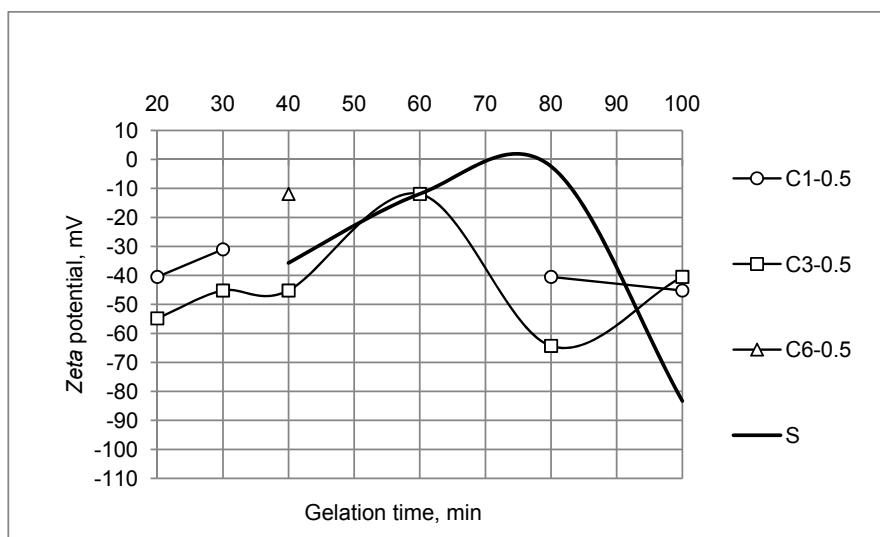


Fig. 30. The second maximum of electrophoretic signal intensity I and corresponding Zeta potential of colloidal particles formed after gelling the "soluble sodium silicate type C1-0.5, C3-0.5, C6-0.5 and S – ester hardener" system

Rys. 30. Drugie maksimum intensywności sygnału elektroforetycznego I oraz odpowiadający mu potencjał Zeta cząstek koloidalnych powstających w żelującym układzie „uwodniony krzemian sodu rodzaju C1-0.5, C3-0.5, C6-0.5 i S – utwardzacz estrowy”

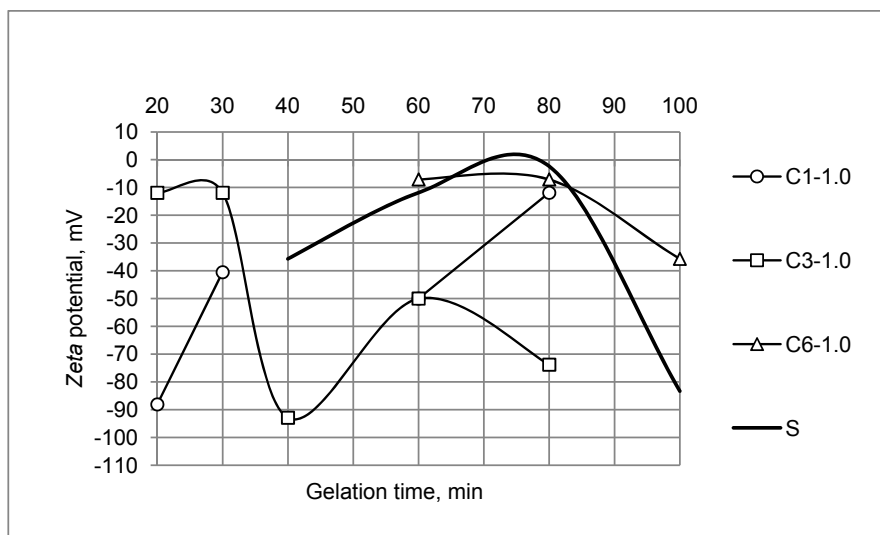


Fig. 31. The second maximum of electrophoretic signal intensity I and corresponding Zeta potential of colloidal particles formed after gelling the "soluble sodium silicate type C1-1.0, C3-1.0, C6-1.0 and S – ester hardener" system

Rys. 31. Drugie maksimum intensywności sygnału elektroforetycznego I oraz odpowiadający mu potencjał Zeta cząstek koloidalnych powstających w żelującym układzie „uwodniony krzemian sodu rodzaju C1-1.0, C3-1.0, C6-1.0 i S – utwardzacz estrowy”

## Results and discussion

For the standard, chemically non-modified soluble sodium silicate S, the change in the *Zeta* potential of particles in a "chemically unmodified soluble sodium silicate – ester hardener" gelling system is different, compared to changes in the *Zeta* potential of particles in a "chemically modified soluble sodium silicate – ester hardener" gelling system. The *Zeta* potential of particles in a "chemically unmodified soluble sodium silicate – ester hardener" gelling system has a very low and virtually constant value (about - 90 mV) for the gelation time from 20 minutes to 60 minutes. After this time of gelation, the stability of the gelling system decreases strongly and continuously.

For the majority of the investigated types of the chemically modified soluble sodium silicate there are two maxima of electrophoretic signal intensity  $I$  on the surface of colloidal particles formed in a gelation process of the "chemically modified soluble sodium silicate – ester hardener" system. A higher value of the first maximum of intensity  $I$  refers almost entirely to the colloidal particles with the lowest value of *Zeta* potential (from about - 20 mV to about -100 mV), as compared to the value of the *Zeta* potential of particles in the second maximum with lower value electrophoretic signal intensity  $I$ .

The distribution of electrophoretic signal intensity  $I$  on the surface of colloidal particles formed in a "chemically modified soluble sodium silicate – ester hardener" system and the corresponding value of *Zeta* potential indicate different stability of the system in function of the gelation time and the amount of chemical modifier introduced. With increasing content of modifier C1, the *Zeta* potential of the particles responsible for the maximum electrophoretic signal intensity  $I$  was increasing. This type of modifier confers high stability to the system after the gelation time of from about 20 minutes to about 30 minutes. In the interval of about 30 minutes to about 60 minutes of the gelling time, the stability of the system is declining. After the gelling time from about 60 minutes to about 100 minutes, the stability of the system recurs once again.

With application of modifier C3, high stability of the system was also reported after the gelling time from about 20 minutes to about 40 minutes. After this gelling time the stability of the system was decreasing, to increase once again after the gelling time of about 80 minutes.

Modifier C6 confers high stability to the system after the gelling time from about 20 minutes to about 40 minutes. After the gelling time from about 40 minutes to about 60 minutes, a decrease in the system stability has been observed. The stability of the system has increased once again after the gelling time from about 60 minutes to about 100 minutes.

## Conclusions

1. An increase in the content of modifiers C1, C3 and C6 will confer more stability to the "chemically modified soluble sodium silicate – ester hardener" system, with the prolonged time of gelation. For the modifier content of 0.1%, 0.5% and 1.0%, the *Zeta* potential of the particles is from about -70 mV to about -90 mV, from about -65 mV to about -95 mV, and from about -45 mV to about -95 mV, respectively, with the gelation time of from about 20 minutes to about 30 minutes, from about 20 minutes

to about 40 minutes, and from about 20 minutes to about 60 minutes. At the same time, the maximum value of the Zeta potential decreases for the above mentioned gelation times of the system.

2. The smallest differences in the stability of the "chemically modified soluble sodium silicate – ester hardener" system for the whole range of the gelation time are provided by modifier C3-0.1 (from about -90 mV to about -65 mV) and by modifier C6-1.0 (from about -75 mV to about -50 mV).
3. All kinds of modifiers, i.e. C1, C3 and C6, confer increased stability to the "chemically modified soluble sodium silicate – ester hardener" system after the gelation time of from about 80 minutes to about 100 minutes.

## Acknowledgement

The results presented in this publication were based on a research conducted under the Target Project No. 6 T09 2003/C.6137 "Starting the production of an environment-friendly inorganic binder of new generation for casting of ferrous and nonferrous metal alloys".

## References

1. Baliński A., Stechman M., Różycka D.: *Influence of modification of the soluble sodium silicate with morphoactive agents on the mechanical properties of the moulding sands in temperatures to 900°C*. Materials Engineering, 2003, Vol. X, No. 3, pp. 271–273.
2. Stechman M., Różyccka D., Baliński A.: *Modification of Aqueous Sodium Silicate Solutions with Morphoactive Agents*. Kongres Te-Chem, Szczecin, 2003.
3. Stechman M., Różyccka D., Baliński A.: *Modification of Aqueous Sodium Silicate Solutions with Morphoactive Agents*. Polish Journal of Chemical Technology, 2003, Vol. 5, No. 3, pp. 47–50.
4. Iler R.K.: *The Chemistry of Silica Solubility. Polymerization. Colloid and Surface Properties and Biochemistry*. Wiley-Interscience, New York, 1979.
5. Kisielev A.V. et al: *Surface Chemical Compounds and their Role in Adsorption*. Moscow State University Press, Moscow, 1957.
6. James R.O., Parks G.A.: *Characterization of aqueous colloids by their electrical double-layer and intrinsic surface chemical properties*. [In:] *Surface and Colloid Sci.*, New York, Wiley Interscience, 1982.
7. Baliński A., Janusz W.: *Potencjał ζ uwodnionego krzemianu sodu*. Archives of Foundry, 2004, Vol. 4, No. 11, pp. 29–33.
8. Baliński A., Janusz W.: *Changes of potential  $\zeta$  in a system of “hydrated sodium silicate – ethylene glycol”*. Advances In Technology of Machines and Mechanical Equipment, 2002, Vol. 26, No. 4, pp. 21–25.
9. Janusz W.: *Electrical double layer at the metal oxide/electrolyte interface*. [In:] J.P. Hsu, Interfacial Forces and Fields, Theory and application. *Surfactant Sci.*, Vol. 85, Chapter 4, New York, 1999.

10. Paszkiewicz M., Pałkowski W.: *Potencjał ξ. Wyznaczanie punktu IPE – ćwiczenie 5.* Zakład Radiochemii i Chemii Koloidów UMCS, 2008.
11. Westall J, Hohl H.: *A comparison of electrostatic model for the oxide/solution interface.* Adv Colloid Interface Sci., 1980, No. 12, pp. 265–294.
12. James R.O.: *Surface ionization and complexation at the colloid/aqueous electrolyte interface.* [In:] Adsorption of Inorganic at Solid/Liquid Interfaces. Ann Arbor, MI: Ann Arbor Sci., 1981, pp. 219–26.
13. Yates D.E., Levine S., Healy T.W.: *Site-Binding Model of the Electrical Double Layer at the Oxide/Water Interface.* J. Chem. Soc. Faraday Trans., 1974, Vol. 70, No. 1807.
14. Davis J.A., James R.O., Leckie J.O.: *Surface Ionization and Complexation at the Oxide/Water Interface. I. Computation of Electrical Double Layer Properties in Simple Electrolytes.* J. Colloid Interface Sci., 1978, Vol. 63, No. 480.
15. Kallay N., Sprycha R., Tomić M., Žalac S., Torbić Ž.: *Some controversies in the understanding of equilibria in electrical interfacial layer.* Croatica Chemica Acta, 1990, No. 63, pp. 467–487.
16. Hunter R.O.: *Zeta Potential in Colloid Science.* Academic Press, London, 1981.
17. Minor M., Van der Linde A.J., Van Leeuwen H.P., Lyklema J.: *Dynamic Aspects of Electrophoresis and Electroosmosis: A New Fast Method for Measuring Particle Mobilities.* J. Colloid Interface Sci., 1997, No. 189, pp. 370–375.
18. Kosmulski M., Hartikainen J., Maczka E., Janusz W., Rosenholm J.B.: *Multiinstrument Study of the Electrophoretic Mobility of Fumed Silica.* Analytical Chem., 2002, No. 74, pp. 253–256.
19. Parks G.A.: *The Isoelectric Point of Solid Oxides, Solid Hydroxides, and Aqueous Hydroxo Complex Systems.* Chem. Rev., 1965, No. 65, pp. 177–198.